

# Development of a Fiber based Interferometric Sensor for Non-contact Displacement Measurement

S. Pullteap

**Abstract**—In this paper, a fiber based Fabry-Perot interferometer is proposed and demonstrated for a non-contact displacement measurement. A piece of micro-prism which attached to the mechanical vibrator is served as the target reflector. Interference signal is generated from the superposition between the sensing beam and the reference beam within the sensing arm of the fiber sensor. This signal is then converted to the displacement value by using a developed program written in visual C++ programming with a resolution of  $\lambda/8$ . A classical function generator is operated for controlling the vibrator. By fixing an excitation frequency of 100 Hz and varying the excitation amplitude range of 0.1 – 3 Volts, the output displacements measured by the fiber sensor are obtained from 1.55  $\mu\text{m}$  to 30.225  $\mu\text{m}$ . A reference displacement sensor with a sensitivity of  $\sim 0.4 \mu\text{m}$  is also employed for comparing the displacement errors between both sensors. We found that over the entire displacement range, a maximum and average measurement error are obtained of 0.977% and 0.44% respectively.

**Keywords**—Non-contact displacement measurement, extrinsic fiber based Fabry-Perot interferometer, interference signal, zero-crossing fringe counting technique.

## I. INTRODUCTION

NON contact measurement is an excellent technique for preventing the target surface due to the surface scratching (touching of a sensing probe and target surface). Several advantages of this technique have been reported in terms of non-destructive surface, hazards measuring, and access to difficult areas [1]-[3]. Fiber optic interferometer (FOI) is an interested transducer type which operated on the non-contact measurement [4]. This sensor is generally used for measuring the vibration, stress and strain, temperature, acoustic, etc [5]-[7]. It can be classified into two groups, two beam and multiple-beam interferometers. Fiber based Mach-Zehnder, Sagnac and Michelson interferometers are the first group of the fiber sensor which the sensing arm and the reference arm have been isolated. Interference signal is generated from the superposition between the sensing signal (output signal from the sensing arm) and the reference signal (output signal from the reference arm) correlated to the optical path difference. Several applications use these sensors for rotation, displacement, and pressure measurements [8]-[10].

Fiber based Fabry-Perot interferometer is next represented in the second group. More advantages of this sensor over the two beam interferometer are exploited in terms of reducing the optical devices due to it doesn't require the reference arm, twice times of the resolution cause double reflections generated at the Fabry-Perot etalon, and simply to implement [11]. An extrinsic fiber based Fabry-Perot interferometer (EFFPI) is a typical of the Fabry-Perot interferometer which the sensing signal is generated outside of the fiber sensor. With simplify to implement therefore, it was often employed for non-contact measurements such as acoustic, temperature, displacement, or pressure measurements [12]-[15].

In previous work, the EFFPI sensor was developed for small displacement measurement with a resolution of  $\lambda/2$  under using a simple fringe counting technique [16]. In this paper, the fiber sensor is next employed for the non contact displacement measurement with the resolution of  $\lambda/8$ . Moreover, a developed program written in visual C++ programming with correlated to the zero-crossing fringe counting technique is employed for demodulating the interference signal into displacement value. A reference displacement sensor with a sensitivity of  $\sim 0.4 \mu\text{m}$  is used for investigating the measurement errors and also studying the performance of the sensor for non-contact displacement measurement in various displacements.

## II. OPERATING PRINCIPLE OF EXTRINSIC FIBER BASED FABRY-PEROT INTERFEROMETER

The EFFPI here is considered as a two-beam device due to the relatively poor reflectivity ( $\sim 34\%$ ) of the sensing surface employed. It consists of an optical fiber serving as the sensing arm where a certain amount of the propagating lightwave is reflected at the fiber-air interface to result in a reference signal which can be detected by a photodetector at the output fiber arm. However, the rest of lightwave (approximately 96%) is then transmitted into the target surface and next reflected back into the fiber arm as sensing signal. Interference signal is generated within the fiber arm and then propagated into the output fiber arm through a fiber coupler. Optical path difference between two beams (sensing and reference signals) is used to assume the amplitude of the interference signal (constructive or destructive interference signal). The output intensity of interference signal ( $I$ ) at the output fiber arm is generally given by

Manuscript received February 26, 2010.

Saroj Pullteap is with Department of Mechanical Engineering, Faculty of Engineering and Industrial Technology, Silpakorn University (Sanam Chandra Palace Campus), Nakhon Phathom, Thailand (e-mail: pullteap@hotmail.com).

$$I = I_1 + I_2 + 2\sqrt{I_1 I_2} \cos \Delta\phi \quad (1)$$

where:  $I_1$  and  $I_2$  = intensities of reference and sensing signals  
 $\Delta\phi = \phi_r - \phi_s$  = phase difference between both signals

According to (1), it implies that the output intensity of interference signal is corresponding to the phase difference ( $\Delta\phi$ ) between two beams ( $\phi_r$  and  $\phi_s$ ). Moreover,  $\Delta\phi$  can also be considered from the cavity length ( $L$ ) between the fiber end and the target as followed by [17]:

$$\Delta\phi = \frac{4\pi n \Delta L}{\lambda} \quad (2)$$

where  $\lambda$  is the injected wavelength,  $n$  corresponds to the refractive index of light in media ( $n = 1$  in air), and  $\Delta L$  is twice times of the cavity length variation. A simple structure of EFFPI sensor can be shown in figure 1.

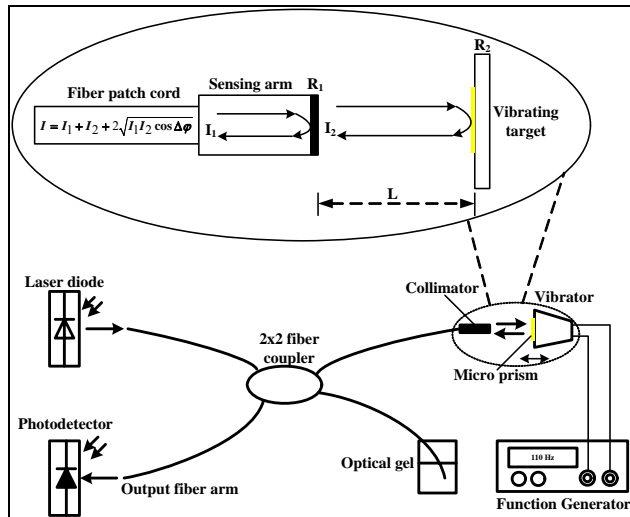


Fig. 1 Operating principle of extrinsic fiber based Fabry-Perot interferometric sensor

Monochromatic light from the laser diode source is injected the light into a single-mode fiber pigtailed. This beam is next propagated through a 2x2 fiber coupler and then split into two beams. One is propagated into the fiber clave-end while the other is injected into an optical gel for reducing or eliminating the reflection losses. Considering to the fiber end, approximately 4% of light is reflected off at the air interface ( $R_1$ ) which is called "reference signal" while the remaining light is next propagated through air cavity ( $L$ ) with a second reflection occurring at the target ( $R_2$ ) called as "sensing signal". Two reflective signals (reference and sensing signals) interfere constructively and destructively based on the optical path difference which is called the "interference signal". It is next propagated to the output arm of the fiber interferometer and then converted into the electrical quantity by a

photodetector. This signal is directly proportioning to the target movement (changing in the cavity length) which is controlled by a classical function generator. In addition, it has to be demodulated into a physical quantity (temperature, pressure, or displacement) by using a simple demodulation technique such as fringe counting or phase tracking technique [18]-[19]. In this work, a simple fringe counting technique is employed for demodulating the displacement information of the target movement which can thus be calculated by [18]

$$D = N \frac{\lambda}{2} \quad (3)$$

where  $D$  represents the displacement of the vibrating target,  $N$  is the number of the interference fringe, and  $\lambda$  is the injected wavelength respectively.

According to (3), the resolution of the system is generally achieved of  $\lambda/2$  due to it usually count only a peak of the interference fringe. However, to increase the resolution more than that, the fringe analysis techniques [18]-[19] have to be operated for obtaining the number of interference fringe more than 1 point per fringe.

### III. DEMODULATION BY ZERO-CROSSING FRINGE COUNTING TECHNIQUE

This section presents a demodulation technique for obtaining the resolution of  $\lambda/8$ . By increasing the fringe counting number from 1 to 4 points per time period, the resolution as considered can be achieved. To do this process, a bucket-bin method correlated with a zero-crossing fringe counting technique [20] are proposed as shown the expression by

$$V_{mean} = \frac{(V_{max} + V_{min})}{2} \quad (4)$$

where  $V_{mean}$ ,  $V_{max}$ , and  $V_{min}$  are the mean, maximum, and minimum voltages of interference signal detected by the photodetector. In addition, the expression of zero-crossing fringe counting technique is followed by [21]

$$X_l = \frac{V_{mean} - V(X_{lb})}{V(X_{la}) - V(X_{lb})} + X_{la} \quad (5)$$

$$X_r = \frac{V_{mean} - V(X_{rb})}{V(X_{rb}) - V(X_{ra})} + X_{rb} \quad (6)$$

where  $X_l$  and  $X_r$  are the crossover points on the left and right sides of the interference fringe while  $V(X_{lb})$ ,  $V(X_{rb})$ ,  $V(X_{la})$ , and  $V(X_{ra})$  are the interference voltages of the crossover points on both sides at above and below of  $V_{mean}$  position respectively. Consequently,  $X_{la}$  is the last pixel of  $V(X_{la})$  over  $V_{mean}$ , and  $X_{rb}$  is the first pixel of  $V(X_{rb})$  below  $V_{mean}$  position.

Figure 2 shows a simulated interference signal correlated to the demodulation technique as mentioned above written in Visual C++ programming.

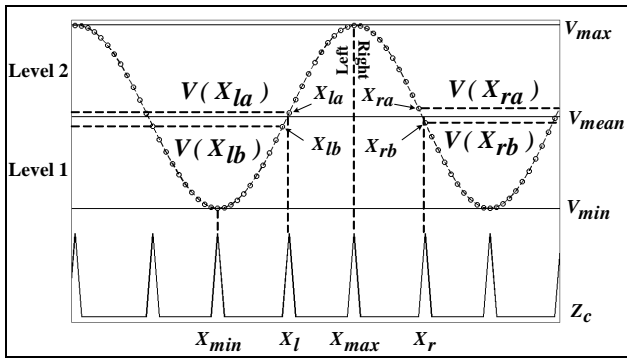


Fig. 2 Demodulation technique for increasing resolution of EFFPI sensor by using bucket-bin correlated with zero-crossing fringe counting

To obtain 4 points/time period, the maximum and minimum values of interference fringe have to be considered. These values obtain  $X_{min}$  and  $X_{max}$  positions as shown in figure 2. In addition, a mean value ( $V_{mean}$ ) of interference fringe is next investigated. By using (4), this value can thus be exploited. Hence, there are two positions now are counted. However, the rest of two positions still investigated. To do that the zero-crossing fringe counting technique as shown in (5) and (6) are used. The concept of this technique is counting the point which crossing over  $V_{mean}$ . As shown in figure 2, the detected voltage of two separated positions are crossed over the mean value called as "left and right sides ( $V(X_{la})$  and  $V(X_{ra})$ ". By using (5) and (6), the two zero-crossing points ( $Z_c$ ) on the both sides of interference fringe ( $X_l$  and  $X_r$ ) can be obtained. These values are then recombined to the  $X_{min}$ ,  $X_{max}$  values leads to 4 zero-crossing points/time period or equivalent to the resolution of  $\lambda/8$ . A block diagram of the demodulation technique via a developed programming can be shown in figure 3.

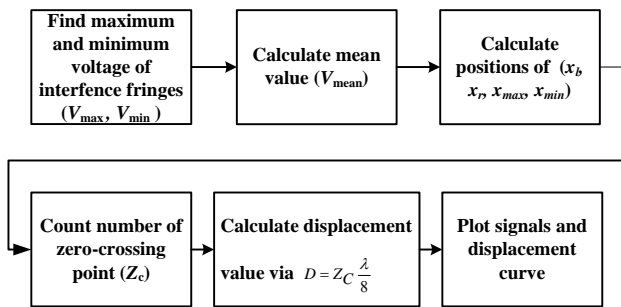


Fig. 3 Block diagram of demodulation technique using bucket-bin correlated with zero-crossing fringe counting

As shown in figure 3, a developed program written in visual C++ programming is employed for investigating the displacement information via the demodulation technique. The operation of this program is first finding the maximum and minimum values of the interference fringe for obtaining  $V_{max}$  and  $V_{min}$  which are detected by the photodetector. Consequently, it's next using the bucket-bin method for

calculating  $V_{mean}$  and then using (5) and (6) for finding the crossover points which is indicated over  $V_{mean}$ . Four zero-crossing points/time period ( $Z_c$ ) of the interference fringe are counted by the program. The displacement value ( $D$ ) now is calculated by multiplying the number of zero-crossing points ( $Z_c$ ) with  $\lambda/8$ . Finally, the displacement curve and the related signals are then plotted on the monitor.

#### IV. EXPERIMENTS AND RESULTS

The experimental setup of the EFFPI sensor for non-contact displacement measurement can be divided into two main parts: hardware and software. The first part represents the development of EFFPI sensor while the second part is developing of a software programming for demodulating the output interference signal into displacement value with the resolution of  $\lambda/8$ .

Let first considering the hardware part, the experimental setup of the fiber sensor for small displacement measurement can be shown its structure in figure 4.

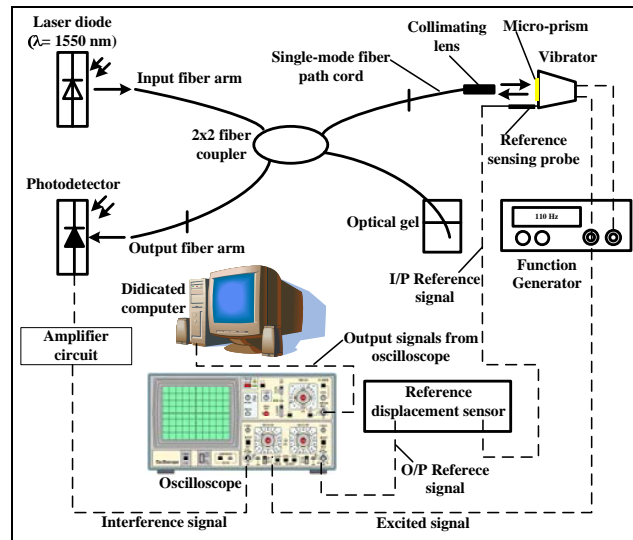


Fig. 4 Experimental setup of EFFPI sensor for non-contact displacement measurement

Monochromatic lightwave from a single-mode fiber pigtailed laser (*LASERMATE*) with a wavelength of 1550 nm, integrating an optical isolator for eliminating back-reflections into the laser source, is injected into the input fiber arm. The light is next propagated into a 2x2 fiber coupler and split into two beams: one is propagated into an optical gel and the other is injected into the sensing arm. 4% of the beam is corresponding to the reference signal which is reflected off at the fiber end while the 96% of the beam is transmitted to the target and then reflected back into the fiber arm as the sensing signal. Interference signal is thus generated within the fiber arm and next propagated into the output fiber arm through the fiber coupler. This signal is then converted into the electrical quantity (voltage) by the photodetector. In general, the output signal obtained from the detector is very small (approximately 20 mV), therefore it has to be amplified before transferred to

display on the oscilloscope, or interfaced to a dedicated computer. As mentioned in section II, the number of interference fringe, in generally, is directly proportioning to the target movement. Hence, when the amplitude of the vibrator is increased by the classical function generator leads to the increment of target displacement as well.

In previous work [16], the variation range of excitation frequency from 2 Hz to 1.5 kHz has been investigated. We found that at  $\sim 50$  Hz and 5 volts for excitation amplitude, a maximum displacement of  $96.01 \mu\text{m}$  was obtained. In this work, the performance of the fiber sensor for small displacement measurement is next studied. A developed program written in Visual C++ programming is employed for demodulating the displacement value with a resolution of  $\lambda/8$  via the uses of zero-crossing fringe counting technique. Moreover, a reference displacement sensor (*Keyence model EX305V*) with a sensitivity  $\sim 0.4 \mu\text{m}$  is also employed for comparing the obtained data from the EFFPI sensor. A sample interference signal measured by the fiber interferometer correlated with a reference signal on the oscilloscope are shown in figure 5

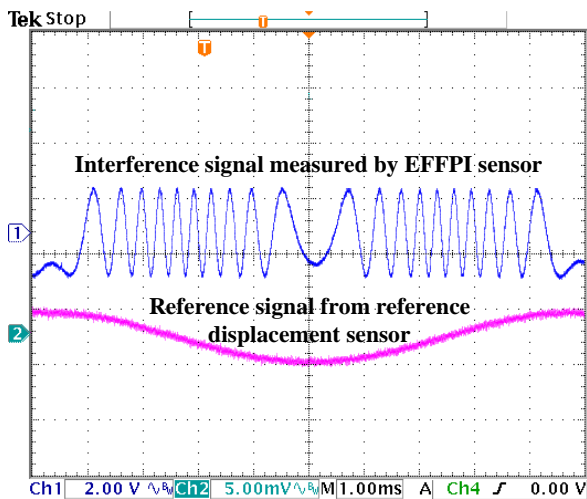


Fig. 5 Output interference signal obtained from EFFPI sensor and reference signal measured by reference displacement sensor at 100 Hz for excitation frequency and 800 mV for excitation amplitude

By fixing the excitation frequency of 100 Hz with 800 mV for excitation amplitude, the output interference signal obtained from the fiber sensor is shown in figure 5. A displacement value of  $7.55 \mu\text{m}$  was obtained by using a simple fringe counting technique with the resolution of  $\lambda/2$  ( $N = 10$ ) while the reference displacement sensor was detected a displacement of  $7.22 \mu\text{m}$  respectively. This gives a measurement percentage error of 4.57%. According to this result, it implies that a simple fringe counting technique as used in previous work is usually not accurate due to it counts only the interference peak. However, when the demodulation technique as mentioned before is employed, the output interference signal and the displacement curve with resolution of  $\lambda/8$  are then plotted in figure 6.

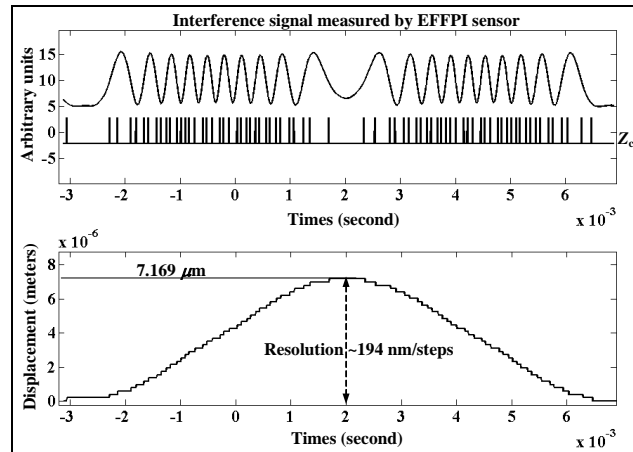


Fig. 6 Output interference signal and displacement curve plotted by developed program with resolution of  $\lambda/8$

With the same configuration as mentioned above, a displacement of  $7.169 \mu\text{m}$  was obtained by the fiber sensor while the output displacement from the reference displacement sensor still detected at the same value ( $7.22 \mu\text{m}$ ) leads to a measurement percentage error of 0.71%. This clarifies that the measurement error can thus be reduced when using the zero-crossing fringe counting technique. However, when the excitation amplitude is varied from 0.1 to 3 volts in steps of 100 mV, the output displacements can be summarized and plotted in figure 7.

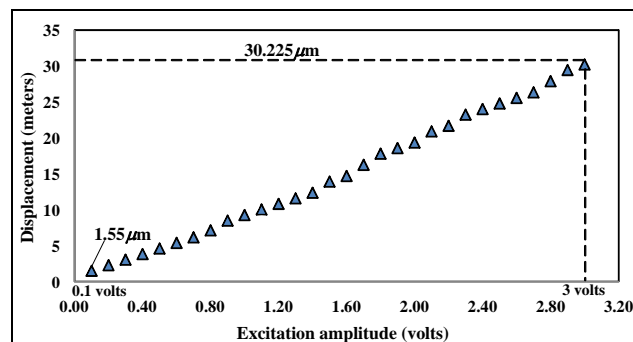


Fig. 7 Relationship between excitation amplitude and output displacement measured by EFFPI sensor

Considering to the experimental data in figure 7, a minimum and maximum displacement of  $1.55 \mu\text{m}$  (for 0.1 volts) and  $30.225 \mu\text{m}$  (for excitation amplitude of 3 volts) are obtained. This confirms that the increment of displacement information is directly proportioning to the increment of excitation amplitude. Moreover, the output reference displacements of  $1.54 \mu\text{m} - 30.05 \mu\text{m}$  are achieved over the entire excitation range. By comparing the EFFPI data with the reference data leads to a maximum and average displacement percentage error of 0.977% and 0.44%.

The relationship between displacement values measured by the fiber sensor and reference displacement values from the reference sensor can be summarized and shown in figure 8.

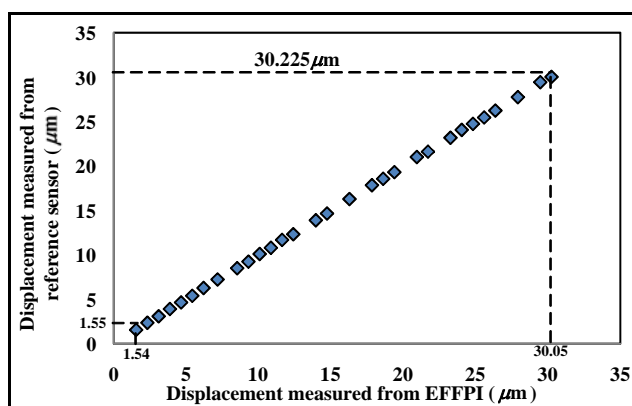


Fig. 8 Relationship between output displacements measured by EFFPI sensor and reference displacements measured by reference displacement sensor

According to the experimental results in figure 8, it implies that the relative direction of the output displacements measured by both sensors is correlated and a trend line of this graph is almost linear. This result confirms the excellent performance of the EFFPI for non-contact displacement measurement in various displacement ranges.

#### V. CONCLUSIONS

The fiber optic based Fabry-Perot interferometer has been developed for non-contact displacement measurement in this paper. A mechanical vibrator attached with a piece of micro-prism was used as the target's reflector. By fixing the excitation frequency of 100 Hz and varying the excitation amplitude from 0.1 to 3 volts by a classical function generator, the displacement amplitudes of 1.55 – 30.225  $\mu\text{m}$  have been achieved. These values were generally demodulated by a developed program written in Visual C++ correlated to the resolution of  $\lambda/8$ . To study the accuracy of the fiber sensor, the reference displacement sensor was employed for the data comparison. We found that the maximum percentage displacement error was obtained of 0.977% over the entire displacement range. This error would be exploited from the misalignment of the experimental setup, environmental influence, or the noise signals from the amplifier circuits etc.

#### ACKNOWLEDGMENT

Author thanks Professor Thierry Bosch and Associate Professor Han Cheng Seat from INP Toulouse France for giving an ideal of the Extrinsic Fiber based Fabry-Perot interferometer.

#### REFERENCES

[1] C. F. Yen and M. C. Chu, "Noncontact measurement of nerve displacement during action potential with a dual-beam low-coherence interferometer," *Opt. Lett.*, vol. 2, no. 17, pp. 2028-2030, 2004.  
 [2] F. J. He, R.J. Zhang, Z. J. Du, and X. M. Cui, "Non-contact Measurement of Damaged External Tapered Thread Based on Linear Array CCD," *Journal of Physics*, conference series 48, pp. 676-680, 2006.

[3] J. Gao, J. Folkes, O. Yilmaz and, N. Gindy, "Investigation of a 3D non-contact measurement based blade repair integration system," *Journal of Aircraft Engineering and Aerospace Technology*, vol. 77, issue 1, pp. 34-41, 2005.  
 [4] E. UDD (Ed.), "Fiber Optic Sensor: An Introduction for Engineers and Scientists," Wiley & Sons Inc., New York, 1991.  
 [5] W. J. Bock, M. S. Nawrocka and W. Urbanczyk, "Coherence-multiplexed fiber optic sensor systems for measurements of pressure and temperature changes," *IEEE Trans. Instrum. Measure.*, vol. 51, no. 5, pp. 980-984, 2002.  
 [6] D. A. Jackson, "Monomode optical fibre interferometers for precision measurement," *J. Phys. E: Sci. Instrum.*, vol. 18, pp. 981-1001, 1985.  
 [7] H. S. Park, G. Thursby and B. Culshaw, "Optical acoustic detector based on a fiber Fabry-Perot interferometer," *Appl. Opt.*, vol. 44, no. 4, pp. 489-492, 2005.  
 [8] V. Louis, P. L. Huy, J. M. Andre, M. Abignoli, and Y. Granjon, "Optical fiber based sensor for angular measurement in rehabilitation," *IEEE Proc. System, Man, and Cybernetics*, vol. 5, pp. 153-157, 1993.  
 [9] B. J. Halkon and S. J. Rothberg, "Vibration measurements using continuous scanning laser Doppler vibrometer: theoretical velocity sensitivity analysis with applications," *Meas. Sci. Technol.*, vol. 14, pp. 382-393, 2003.  
 [10] K. Weir, W. J. O. Boyle, B. T. Meggitt, A. W. Palmer and K. V. T. Grattan, "A novel adaptation of the Michelson interferometer for measurement of vibration," *IEEE J. Lightw. Technol.*, vol. 10, no. 5, pp. 700-703, 1992.  
 [11] J. M. Vaughan, *The Fabry-Perot interferometer: History – Theory – Practice and Applications*, Taylor & Francis, 1989.  
 [12] T. K. Gangopadhyay and P. J. Henderson, "Vibration : history and measurement with an extrinsic Fabry-Perot interferometer sensor with solid-state laser interferometry," *Appl. Opt.*, vol. 38, no. 12, pp. 2471-2477, 1999.  
 [13] N. Singh, S. C. Jain, A. K. Aggarwal and R. P. Bajpai, "Develop and experiment studies of fibre optic extrinsic Fabry-Pérot interferometric sensor for measurement of strain in structures," *Current Science*, vol. 86, no. 2, pp. 309-314, 2004.  
 [14] T. K. Gangopadhyay, S. Chakravorti, K. Bhattacharya and S. Chatterjee, "Wavelet analysis of optical signal extracted from a non-contact fibre-optic vibration sensor using an extrinsic Fabry-Pérot interferometer," *Meas. Sci. Technol.*, no. 16, pp. 1075-1082, 2005.  
 [15] M. Han and A. Wang, "Exact analysis of low-finesse multimode fibre extrinsic Fabry-Perot interferometers," *Appl. Opt.*, vol.43, no. 24, pp. 4659-4666, 2004.  
 [16] N. Sathitanon, and S. Pullteap, "A fiber optic interferometric sensor for dynamic measurement," *International Journal of Computer Science and Engineering*, vol. 2, pp. 63 –66, 2008.  
 [17] K. V. T. Grattan and B. T. Meggitt, *Optical Fiber Sensor Technology Volume 2 : Devices and Technology*, Chapman & Hall, 1998.  
 [18] T. K. Gangopadhyay, "Non-contact vibration measurement based on extrinsic Fabry-Perot interferometer implemented using arrays of single-mode fibres," *Meas. Sci. Technol.*, vol. 15, no. 5, pp. 911-917, 2004.  
 [19] M. Servin, J. L. Marroquin, and F. J. Cuevas, "Demodulation of a single interferogram by use of a two-dimensional regularized phase-tracking technique," *Appl. Opt.*, vol. 36, no. 19, pp. 4540-4548, 1997.  
 [20] A. Choudry, "Digital holographic interferometry of convective heat transport," *Appl. Opt.*, vol. 20, no. 7, pp. 1240-1244, 1981.  
 [21] S. Pullteap, H. C. Seat and T. Bosch, "Modified fringe-counting technique applied to a dual-cavity fiber Fabry-Perot vibrometer," *Opt. Eng.*, vol. 42, no. 11 pp. 15563/1- 8, 2007.